論文 한국공작기계기술학회지 제 6 권 제 4 호 1997. 12.
Journal of the Korean Society of Machine Tool Engineers

열처리시 발생되는 잔류응력이 금속복합체에 미치는 영향에 관한 실험 및 수치해석적 연구

김 홍 건*

An Experimental and Numerical Study on the Thermally Induced Residual Stress Effect in Metal Matrix Composites

Kim Hong Gun*

Abstract

A continuum analysis has been performed for the application to the thermo-elasto-plastic behavior in a discontinuous metal matrix composite. An FEM (Finite Element Method) analysis was implemented to obtain the internal field quantities of composite as well as overall composite behavior and an experiment was demonstrated to compare with the numerical simulation. As the procedure, a reasonably optimized FE mesh generation, the appropriate imposition of boundary condition, and the relevant postprocessing such as elastoplastic thermomechanical analysis were taken into account. For the numerical illustration, an aligned axisymmetric single fiber model with temperature dependent material properties and precipitation hardening effect has been employed to assess field quantities. It was found that the residual stresses are induced substantially by the temperature drop during thermal treatment and that the FEM results of the vertically and horizontally constrained model give a good agreement with experimental data.

Keywords : Residual Stress (잔류응력), Short Fiber Metal Matrix Composite(SFMMC: 단섬유 금속복합체), Reinforcement (보강재), Coefficient of Thermal Expansion (CTE: 열팽창계수), Thermo-elasto-plastic(열탄소성)

1. INTRODUCTION

Recently, Short Fiber Reinforced Metal Matrix Composites (SFMMCs) have been extensively investigated because it is more economical to produce economic production of SiC fibers

* 전주대학교 기계공학과

(whiskers), which has also led to the use of platelet or particulate SiC in Metal Matrix Composites (MMCs). One of the advantages of discontinuous composite is that they can be shaped by standard metallurgical processes such as forging, rolling, extrusion, and so forth.[1-3]

It is well known that certain processing operations introduce residual stresses. These may be caused by combined mechanical and thermal effects, or by surface diffusion treatments such as nitriding. Some processes induce compressive residual stresses and others tensile residual stresses. Thus, some may be beneficial and others detrimental to the strength.

In SFMMCs, where the matrix and reinforcements are well bonded, thermally induced significant residual stresses can arise due to Coefficient of Thermal Expansion (CTE) mismatch between two constituents.[3-8] In fact, residual stresses are the system of stresses which can exist in a body when it is free from external forces. They are sometimes referred to as "internal stresses" or "locked-in stresses". Therefore, it can be mentioned that accurate prediction of the magnitude and distribution of residual stress is crucial to the design and analysis of MMCs. In recent numerical studies,[8,9] it was shown that the magnitude of thermal residual stress is significant, adequate to result in substantial plastic yielding around fibers after cooling from the processing temperature though the age hardening effect was neglected.

Many studies have been reported to predict the overall stress-strain responses including residual stress effects. However, a crucial point to investigate the residual stresses is to simulate the material properties as temperature-dependent behavior, which gives a lot more accurate results compared to temperature-independent behavior.

In this paper, the more detailed study considering temperature dependent material properties and precipitation hardening effect were performed. An axisymmetric finite element analysis (FEA) based on incremental plasticity theory using von Mises yield criterion and Plandtl-Reuss equations was implemented to evaluate properties of the representative volume element (RVE) with and without residual stresses. Numerically predicted tensile stress-strain behaviors were also compared to the experimental results and the role of residual stress was discussed in detail. It was found that the residual stress strongly effects on the localized deformation evolution though it is not so sensitive to the macroscopic resultants as the microscopic field quantities.

2. THERMO-ELASTO-PLASTIC FEM FORMULATIONS

The FEM formulations in this work are centered on the thermo-elasto-plastic analysis with small strain plasticity theory[10] using an axisymmetric single fiber model. The model is based on incremental plasticity theory using von Mises yield criterion, Plandtl-Reuss equations and isotropic hardening rule. The strains here are assumed to develop instantaneously. To solve nonlinearity, Newton-Raphson method has been implemented. Based on the thermomechanical theory,[8,10,11]

$$\{d\varepsilon^{el}\} = \{d\varepsilon\} - \{d\varepsilon^{pl}\} - \{d\varepsilon^{th}\} \quad (1)$$

where $\{d\varepsilon\}$, $\{d\varepsilon^{el}\}$ and $\{d\varepsilon^{pl}\}$, $\{d\varepsilon^{th}\}$ are the changes in total, elastic, plastic and thermal strain vectors, respectively. The thermal strain vector $\{d\varepsilon^{th}\}$ is

$$\{d\varepsilon^{th}\} = \{CTE\}\{\Delta T\} \quad (2)$$

According to von Mises theory, yielding begins under any states of stress when the effective stress σ_e exceeds a certain limit, where

$$\sigma_e = \left[\frac{1}{2}\{(\sigma_x-\sigma_y)^2+(\sigma_y-\sigma_z)^2+(\sigma_x-\sigma_z)^2\} + 3\,(\tau_{xy}^2+\tau_{yz}^2+\tau_{xz}^2)\right]^{1/2} \quad (3)$$

The stress increment can be computed via the elastic stress-strain relations as follows:

$$\{d\sigma\} = [D]\{d\varepsilon^{el}\} = [D](\{d\varepsilon\} - \{d\varepsilon^{pl}\} - \{d\varepsilon^{th}\}) = [D_{ep}]\{d\varepsilon\} \quad (4)$$

where [D] is the elastic stress-strain matrix and $[D_{ep}]$ is the elastoplastic stress-strain matrix which is given by

$$[D_{ep}] = [D]\left(1 - \left\{\frac{\partial Q}{\partial \sigma}\right\}\{C_\lambda\}^T\right) \quad (5)$$

where Q is the plastic potential and $\{C_\lambda\}$ is the factor influencing to the plastic multiplier.

On the other hand, the principle of virtual work says that a virtual (very small) change of the internal strain energy must be offset by an identical change in external work due to the applied loads, i. e.,

$$\delta U = \delta V \quad (6)$$

where U is the strain energy (internal work), V is the external work, and δ is the virtual operator. The virtual strain energy is

$$\delta U = \int_V \{\delta\varepsilon\}^T\{\sigma\}\,dV \quad (7)$$

Equations (6) and (7) are combined to give

$$\delta U = \int_V (\{\delta\varepsilon\}^T[D]\{\varepsilon\} - \{\delta\varepsilon\}^T[D]\{\varepsilon^{th}\})\,dV$$

The strains are related to the nodal displacements by

$$\{\varepsilon\} = [B]\{U\} \quad (9)$$

Combining equation (8) with (9)

$$\delta U = \{\delta U\}^T\int_V [B]^T[D][B]\,dV\,\{u\} - \{\delta U\}^T\int_V [B]^T[D]\{\varepsilon^{th}\}\,dV \quad (10)$$

Next, the external virtual work by nodal forces is

$$\delta V = \{\delta U\}^T\{F_e\} \quad (11)$$

where $\{F_e\}$ is nodal forces applied to the element. On the other hand, component stresses were calculated for each element at its integration points (or Gauss points). The stress values are then extrapolated to the nearest node using element shape functions, resulting in a nodal component stress for that node due to that element. At a node shared by two elements, therefore, we have two nodal stress values, one from each element. In general, the nodal stresses in the entire model are averaged by the stress contributions from all elements shared by a particular node.

3. MODEL

The thermo-elasto-plastic micromechanical model to describe the SFMMCs has been chosen for a single fiber model as used in the previous work.[12-14] In this model, a uniform fiber distribution with an end gap value equal to transverse spacing between fibers was selected. Further, the fibers were assumed as uniaxially aligned with no fiber/matrix debonding allowed for, in keeping with the actual situation in many SFMMCs.[13-16]

The application of FEM to composites requires careful attention to the geometry of the mesh used in analysis and design. In a discontinuous fiber reinforced composite, fiber interaction effects must be important in understanding the deformation evolution in the matrix as well as the overall composite stress-strain behavior except in very low fiber volume fraction cases.[17-20] An axisymmetric single fiber model corresponding to

a 3-D model for the aligned geometry and fiber/fiber interactions can be accounted for by use of vertical and horizontal cell boundary constraining conditions. In this study, an axisymmetric single fiber (RVE) which qualitatively and quantitatively provides the equivalent results as 3-D model was employed as shown in Fig. 1. The spatial variable for the axial (mechanical loading) direction is z with the coordinate origin at the fiber center, whereas the spatial variable for the radial direction is r. For an FE mesh generation, consequently, the quarter of RVE is needed to analyse due to axisymmetry. FE computations were performed using four noded isoparametric elements. The constraint boundary condition enforces elastic and plastic constraint by requiring that the radial and axial boundary of RVE is maintained in the straight manner during deformation.[21-23]

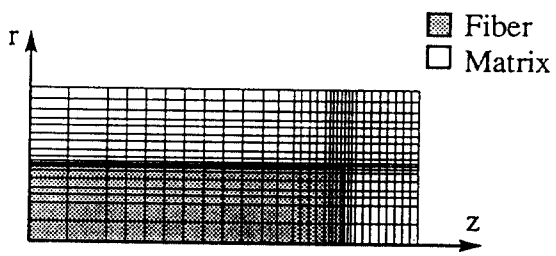

Fig. 1 The RVE and mesh pattern for an axisymmetric single fiber model.

4. EXPERIMENT

To predict the constitutive relations of SFMMCs, tensile stress-strain curves for Al 2124 control alloy and Al 2124 composite reinforced by 20 vol. % SiC whisker were obtained using strain controlled tensile test at the strain rate of 10^{-3}/sec in the Instron 1330 Servo-Hydraulic test machine. The unreinforced Al 2124 was processed in identical fashion to the composite, namely, by a powder metallurgy (PM) process involving hot processing above the solidus followed by hot extrusion. The SiC whiskers were 0.5-1.0μm in diameter with an average aspect ratio of 4 and tended to be aligned in the extrusion direction which corresponds to the longitudinal axis of the tensile samples. After machining, the samples were heat treated for the T-6 condition. Fig. 2 represents the process of residual stress generation in case of the T-6 heat treatment condition.

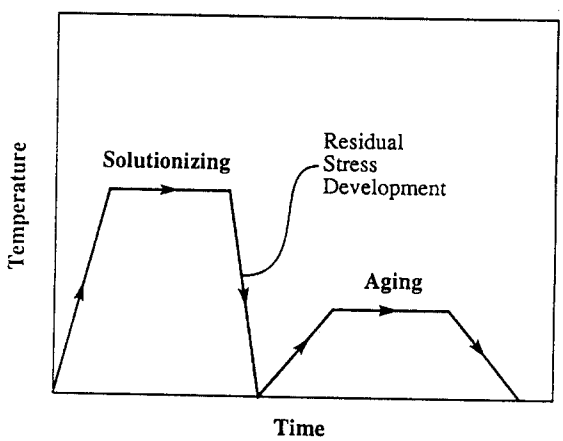

Fig. 2 A Process of residual stress generation in case of the T-6 heat treatment condition.

From these matrix test data, a bilinear representation of the matrix stress-strain curve was obtained for FEA simulation. Thus, stress-strain characteristics of the matrix were defined by the elastic modulus, yield stress and work hardening rate (tangent modulus). These characteristics were measured at room temperature on the PM 2124 Al alloy and were found to be E_m=70GPa, σ_{my}=336MPa and E_T=1.04GPa, respectively. The material properties of high temperature behavior were implemented by the documented data.[24,25] Other material properties chosen were ν_m=0.33 and α_m=2.36x10^{-5}/K for

the matrix and E_f=480GPa, ν_f=0.17 and α_f=4.3x10^{-6}/K for the reinforcement.[21-23] Here, E is Young's modulus, E_T is tangent modulus, σ_{my} is matrix yield stress, ν is Poisson's ratio and α is CTE. Fig. 3 describes the temperature dependency for the matric material property. In Fig. 3, the vertical strengthening at room temperature means the effect of aging process, and σ_{mu} means matrix ultimate stress.

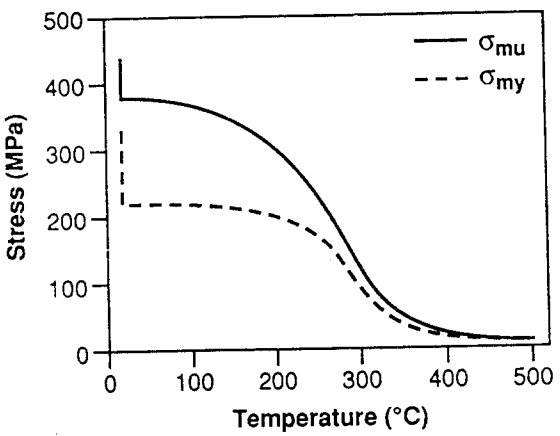

Fig. 3 Temperature dependency of matrix material properties.

5. RESULTS AND DISCUSSION

5.1 Results of Thermo-Elastic Analysis

It is applied to calculate the elastic residual stresses which develop in reinforcing fibers and the matrix during cooling from elevated temperatures. The residual stresses are evaluated as a function of CTE ratio (α_m/α_f), Young's modulus ratio (E_f/E_m) for the volume fraction V_f=20%. In this thermo-elastic analysis, it was found that compressive stresses are produced in the fiber and also in the region between fiber ends as shown in Fig. 4 and 5. This phenomenon is mainly due to constraint effects. Note that this section is limited for the results of thermo-elastic analysis. It is expected that the more significant thermal stresses are produced in case of thermo-elasto-plastic analysis. The results of thermo-elasto-plastic analysis is described in the following sections.

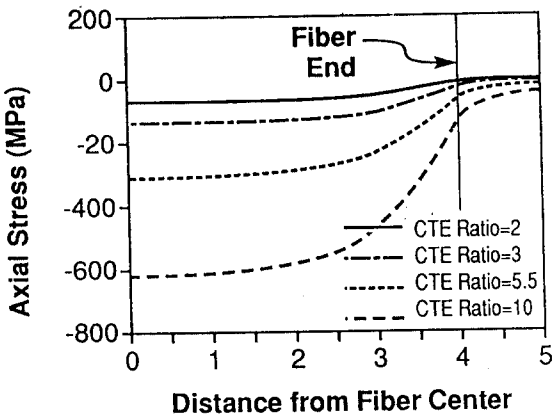

Fig. 4 Fiber thermal stress distribution as a function of α_m/α_f for V_f=20%. The stresses are plotted along the fiber center line.

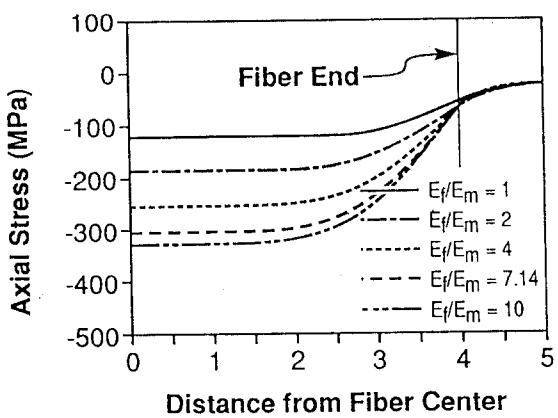

Fig. 5 Fiber thermal stress distribution as a function of E_f/E_m for V_f=20%. The stresses are plotted along the fiber center line.

The magnitudes in the fiber and fiber end gap region are shown in Fig. 4 and 5 as a function of CTE ratio, α_m/α_f and Young's modulus ratio, E_f/E_m. In Fig. 4, α_m/α_f values are varies whereas other material and geometrical parameters are fixed as for the case of SiC(w)/Al system (E_f/E_m=7.14, s=4). In Fig. 5, likewise, E_f/E_m values are varied whereas other conditions are fixed (α_m/α_f=5.5, s=4). It is important to note from these figures that the stresses in the fiber are not constant but show a sigmoidal type of variation that is similar to the stress variation obtained in a shear-lag model when the specimen is loaded mechanically.[22] It is found that, in the figure, the stress patterns are functionally similar for thermal and mechanical loading cases. Note the substantially large fiber and fiber end gap compressive stresses. This further reinforces the equivalence between thermal loading and mechanical loading, and the applicability of a shear-lag approach to quantify the local stresses in both cases.

5.2 Results of Thermo-Elasto-Plastic Analysis

To understand the microscopic behavior, the magnitude and distribution of thermal stress is of interest to investigate the internal stresses. For instance, the thermally induced axial stress and von Mises stress for ΔT=-270K in the matrix are shown in Fig. 5 and 6, respectively. For the axial thermal stress contour, compressive stresses are found in the region between fiber ends whereas tensile stresses are found as expected by axial constraint effects. Likewise, the region between fiber ends shows an extensive deformation because of the combined effect of tensile and compressive constraint conditions as can be seen in Fig. 5. The von Mises stresses due to cooling show that the fiber tip region in the matrix is under the severe condition and that the region between fiber ends in the matrix is also fairly significant condition since constraint effect.

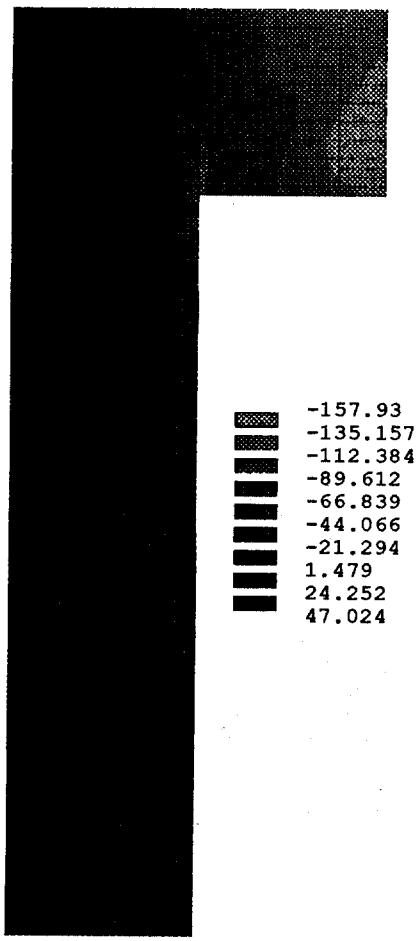

Fig. 6 The typical contour of axial thermal residual stress in the matrix (Unit : MPa).

On the other hand, the fiber or whisker is subjected to substantial compressive stresses in axial direction after cooling, see Fig. 8. Note that the triple fiber model has been implemented to verify an axial constraint. The end-gap stresses in the single fiber model show significantly lower compressive stress values than that for the case

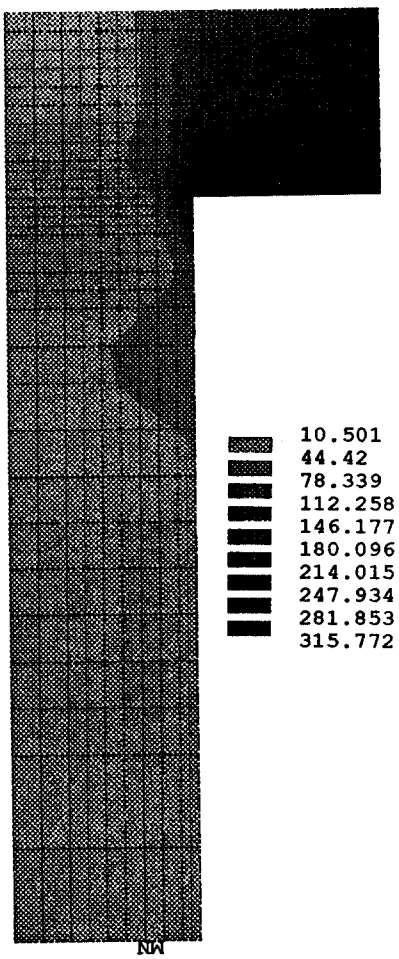

Fig. 7 The typical contour of effective thermal residual stress in the matrix (Unit : MPa).

of the triple fiber model. For example, at ambient temperature the predicted compressive residual stress midway between the fiber end gap is zero for the single fiber model but -152MPa for the triple fiber case. Furthermore, the fiber compressive stresses are also significantly larger in the triple fiber model. This difference represents the role of the constraint effect of the matrix end gap region. The fiber center stresses, however, do not appear to be effected by the end gap constraint. The presence of compressive matrix end gap stresses is an important result not predicted by previous models.[6,7] These stresses would need to be considered in any analysis of failure micromechanisms in these composites.

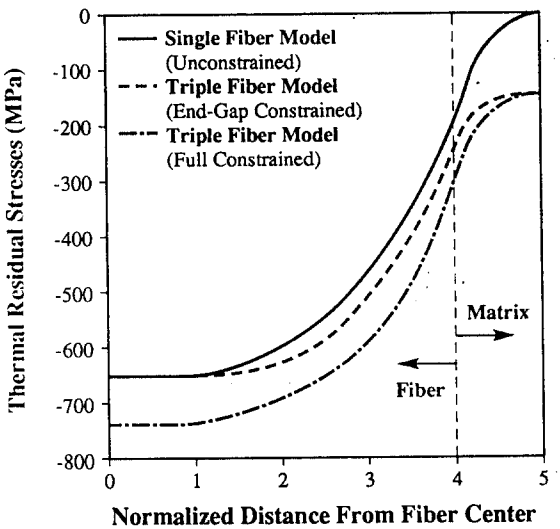

Fig. 8 Thermal residual axial stresses after cooling with and without constraint condition at the fiber center line(Cooled from 773K). Distance from fiber center is normalized with respect to fiber radius.

The matrix surrounding the fiber, on the other hand, is placed under tensile stresses during cooling from elevated temperatures resulting in the formation of a caging plasticity around the SiC fibers or whiskers. Plastic yielding in the matrix begins at elevated temperatures during the cooling process because of the low values of the yield stress at elevated temperatures. The size of the yield zones at lower temperatures is progressively smaller because of the yield stress increase. In fact, this plasticity is large enough to overlap neighboring whiskers. It is important to note that predominantly compressive yield

occurs in the fiber end regions of the matrix in keeping with the compressive stresses in that region.

5.3 Results of the Overall Stress-Strain Response

Fig. 9 represents the dependency of the overall constitutive responses. The figure also includes experimental data to evaluate the role of residual stress effects in the composite. The stress-strain curve with residual stresses is substantially lower than that without residual stresses and also agrees favorably with experimental data. As mentioned in the previous research,[26] the fundamental discrepancy between results calculated and measured tensile properties can be inferred from the deviations in the structure of composite from the idealization of equally spaced cylindrical fibers of identical size, interfacial damage free deformation by perfect bonding assumption and perfectly aligned assumption.[27]

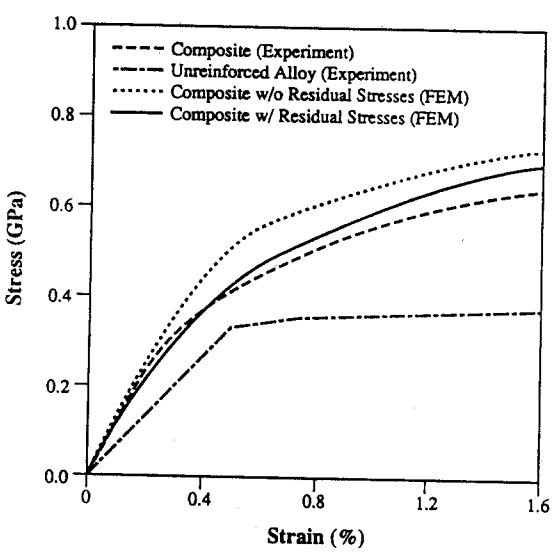

Fig. 9 Stress-strain responses with and without consideration of residual stresses.

Previous FEA results for the stress-strain curve calculated without residual stress also gave higher than experimental values. The discrepancy was attributed to SiC fiber distribution effects. This study suggests that the higher than experimentally observed flow stresses obtained by computation is due in part to the lack of inclusion of residual stresses. The decrease in flow stresses due to the presence of the local residual field is contrary to a previously proposed theory that strengthening in SiC whisker reinforced Al alloy is due to dislocation caging of the SiC whisker after cooling from the elevated temperatures. Any strengthening contribution from dislocation caging effects are offset by a decrease in the composite flow stress as a result directly of the large initial compressive stresses in the fibers and in the matrix end gap regions.

In fact, the enhanced dislocation density model is based upon a contribution to the strengthening from the reflection in an increase in microhardness values for the reinforced matrix. However, this is not observed experimentally for the 2124 SiC whisker composite system.

6. CONCLUSIONS

A thermomechanical(thermo-elasto-plastic) stress analysis was performed to predict the stress-strain tensile respons as well as the local deformation behavior in SFMMCs. It was found that the thermally induced residual stresses are generated substantially and they are sufficient to provide a "caging plasticity" around the stiff fibers. It was also found that the calculated results including residual stresses give more accurate prediction to the experimental data.

7. ACKNOWLEDGEMENT

This work was supported by the 1997 Jeonju University research fund. The author greatly appreciates about the support.

이 논문은 1997년도 전주대학교 학술연구조성비에 의하여 연구되었음.

REFERENCES

1. Gibson, R.A., "Principles of Composite Material Mechanics", McGraw-Hill Inc., pp. 156-189, 1994.
2. Divecha, A.P., Fishman, S.G. and Karmarkar, S.D., "Silicon Carbide Reinforced Alumunum - A Formable Composite", Journal of Metals, pp. 12-17, 1981.
3. Taya, M. and Arsenault, R.J., "Metal Matrix Composites, Thermomechanical Behavior", Pergamon Press, NY., pp. 1-8, 1989.
4. Arsenault, R.J. and Fisher, R.M., "Microstructure of Fiber and Particulate SiC in 6061 Al Composites", Scripta Metallurgica, Vol. 17, pp. 67-71, 1983.
5. Vogelsang, M., Arsenault, R.J. and Fisher, R.M., "An In-Situ HVEM Study of Dislocation Generation at Al/SiC Interfaces in Metal Matrix Composites", Metallurgical Transactions A, Vol. 17A, pp. 379-388, 1986.
6. Taya, M. and Mori, T., "Dislocations Punched-Out around a Short Fiber Metal Matrix Composite Subjected to Uniform Temperature Change", Acta Metallurgica, Vol. 35, No. 1, pp. 155-162, 1987.
7. Derby, B. and Walker, J.R., "The Role of Enhanced Dislocation Density in Strengthening Metal Matrix Composites", Scripta Metallurgica, Vol. 22, pp. 529-532, 1988.
8. Levy, A and Papazian, J.M., "Elastoplastic Finite Element Analysis of Short Fiber Reinforced SiC/Al Composites: Effects of Thermal Treatments", Acta Metallurgica, Vol. 39, No. 10, pp. 2255-2266, 1991.
9. Povirk, G.L., Needleman, A. and Nutt, S.R., "An Analysis of the Effect of Residual Stresses on Deformation and Damage Mechanisms in Al-SiC Composites", Materials Science and Engineering, A132, pp. 31-38, 1991.
10. Cook, R.D., Malkua, D.S. and Plesha, M.E., "Concepts and Applications of Finite Element Analysis, 3rd Edition, John Wiley & Sons, . pp. 163-295, 1989.
11. Taya, M. and Aresenault, R.J., "Metal Matrix Composites : Thermomechanical Behavior," P도-gamon Press, pp. 25-28, 1989.
12. Agarwal, B.D. and Broutman, L.J., "Analysis and Performance of Fiber Composites," John Wiley and Sons, New York, pp. 71-104, 1980.
13. Kim, H.G. and Choe, G.H. "Role of Whisker Stresses in the Deformation and Fracture of Whisker Reinforced Metal Matrix Composites", Proceedings of Korean Society of Composite Materials-Spring Session, pp. 25-30, Apr, 1994.
14. Kim, H.G., "Assessment of Plastic Constraint Effects Induced by Whisker Interactions in Whisker Reinforced Metal Matrix Composites", Journal of the Korean Society of Composite Materials, Vol. 7, No. 3, pp. 1-10, Oct, 1994.
15. Kim, H.G., "An Investigation of the Thermoelastic Behavior in Short Fiber Reinforced Composite Materials", Journal of the Korean Society for Machine Tool Engineers, Vol. 6, No. 3, in press, Sep., 1997.
16. Nair, S.V., Tien, J.K. and Bates, R.C., "SiC Reinforced Aluminum Metal Matrix Composites", International Metals Review, Vol. 30, No. 6, pp. 275-290, 1985.
17. Arsenault, R.J. and Pande, C.S., "Interfaces in Metal Matrix Composites", Scripta Metallurgica, Vol. 18, pp. 1131-1134, 1984.
18. Christman, T., Needleman, A. and Suresh, S., "An Experimental and Numerical Study of Deformation in Metal-Ceramic Composites", Acta Metallurgica, Vol. 37, No. 11, pp. 3029-3050, 1989.

19. Papazian, J.M. and Adler, P.N., "Tensile Properties of Short Fiber Reinforced SiC/Al Composites, Part I. Effects of Metal Matrix Precipitates", Metallurgical Transactions A, Vol. 21A, pp. 401-410, 1990.
20. Levy, A and Papazian, J.M., "Tensile Properties of Short Fiber Reinforced SiC/Al Composites, Part II. Finite-Element Analysis", Metallurgical Transactions A, Vol. 21A, pp. 411-420, 1990.
21. Nair, S.V. and Kim, H.G., "Thermal Residual Stress Effects on Constitutive Response of a Short Fiber or Whisker Reinforced Metal Matrix Composite," Scripta Metallurgica, Vol. 25, No. 10, pp. 2359-2364, 1991.
22. Kim, H.G., "Stress Transfer in Shear Deformable Discontinuous Composites", KSME Journal, Vol. 8, No. 4, pp. 475-484, 1994.
23. Kim, H. G., Chang, S. H., Chang D. S. and Chung, S. K. : "A Numerical Study Using Micromechanics Model for Metal Matrix Composites", Proceedings of Korean Society of Materials-Fall Session, pp. 25-30, Nov, 1994.
24. Phillips, W.L., "Elevated Tempersture Properties of SiC Whisker Reinforced Aluminum", Proceedings of ICCM/2, Edited by Norton, B., pp. 567-576, 1978.
25. 1.Frost, H.J. and Ashby, M.F., "Deformation Mechanism Maps", Pergamon Press, New York, p.21, 1982.
26. Kim, H.G., "Assessment of Plastic Constraint Effects Induced by Whisker Interactions in Whisker Reinforced Metal Matrix Composites," Journal of Korean Society of Composite Materials, Vol. 7, No. 3, pp. 1-10, 1994.
27. Nutt, S.R. and Needleman, A., "Void Nucleation at Fiber Ends in Al-SiC Composites," Scripta Metallurgica, Vol. 21, pp. 705-710, 1987.